

Date of publication xxxx 00, 0000, date of current version xxxx 00, 0000.

Digital Object Identifier 10.1109/ACCESS.2017.DOI

# Preparation of Papers for IEEE ACCESS

HAO LI<sup>1</sup>, (Member, IEEE), SECOND B. AUTHOR<sup>2</sup>, AND THIRD C. AUTHOR, JR.<sup>3</sup>, (Member, IEEE)

<sup>1</sup>Beijing University of chemical and technology, Beijing, 10029 China (e-mail: 2018040206@mail.buct.edu.cn)

<sup>2</sup>Department of Physics, Colorado State University, Fort Collins, CO 80523 USA (e-mail: author@lamar.colostate.edu)

<sup>3</sup>Electrical Engineering Department, University of Colorado, Boulder, CO 80309 USA

Corresponding author: First A. Author (e-mail: author@boulder.nist.gov).

This paragraph of the first footnote will contain support information, including sponsor and financial support acknowledgment. For example, "This work was supported in part by the U.S. Department of Commerce under Grant BS123456."

⋮ **ABSTRACT** blablabla

⋮ **INDEX TERMS** U-Net, Biomedical image segmentation, Attention

## I. INTRODUCTION

**T**HIS document

## II. METHOD

### A. NETWORK ARCHITECTURE

#### B. BOTTLENECK MODULES

在语义分割任务中, deep convolutional layers已经展现出其对提取图像特征的重要性。等人提出了CE-Net [1], 其在Bottleneck采用了DeepLab中的SPP-Block

Backbone	Components	Params	Params size
CE-Net	SAR	135,571,137	517.16
ResU-Net	SAR+ASPP	92,573,377	353.14
ResU-Net	SAR+MRC+RMP	94,669,505	361.14

表 1. Memorize Cost Comparison With Different Methods In Bottleneck

### C. ATTENTION MODULES

## III. EXPERIMENTS

### A. BASELINE AND IMPLEMENTATION

We used a server equipped with an Intel Core i9-9980XE CPU @ 3.00GHz with 64GB RAM and 12GB of RTX2080Ti GPU for our proposed networks training. The operating system of the sever is 64-bits Ubuntu 18.04. The structure

of the network is implemented under the open source deep learning library Pytorch with VSCode implementation.

### B. DATASET

For this study, we conduct our experiments on four differents segmentation tasks. Covering lesions/organs from most commonly used medical imaging modalities including microscopy, computed tomography (CT), and magnetic resonance imaging (MRI). Table III-D1 summarize those datasets in our study.

Dataset	Image	Input Size	Modality	Provider
Cell	30	512 × 512	EM	ISBI 2012 [2]
Liver	4,000	512 × 512	CT	LiTS 2017 [3]
DSB2018	670	256 × 256	EM	Kaggle [4]
COVID19	1,800	630 × 630	CT	Web [5], [6]

表 2. Summaey Of Biomedical Image Segmentation Datasets Used In Our Experiments

a: Cell

The dataset is the segmentation of neuronal structures in electron microscopic recordings. The dataset is provided by the EM segmentation challenge [2] that is started at ISBI

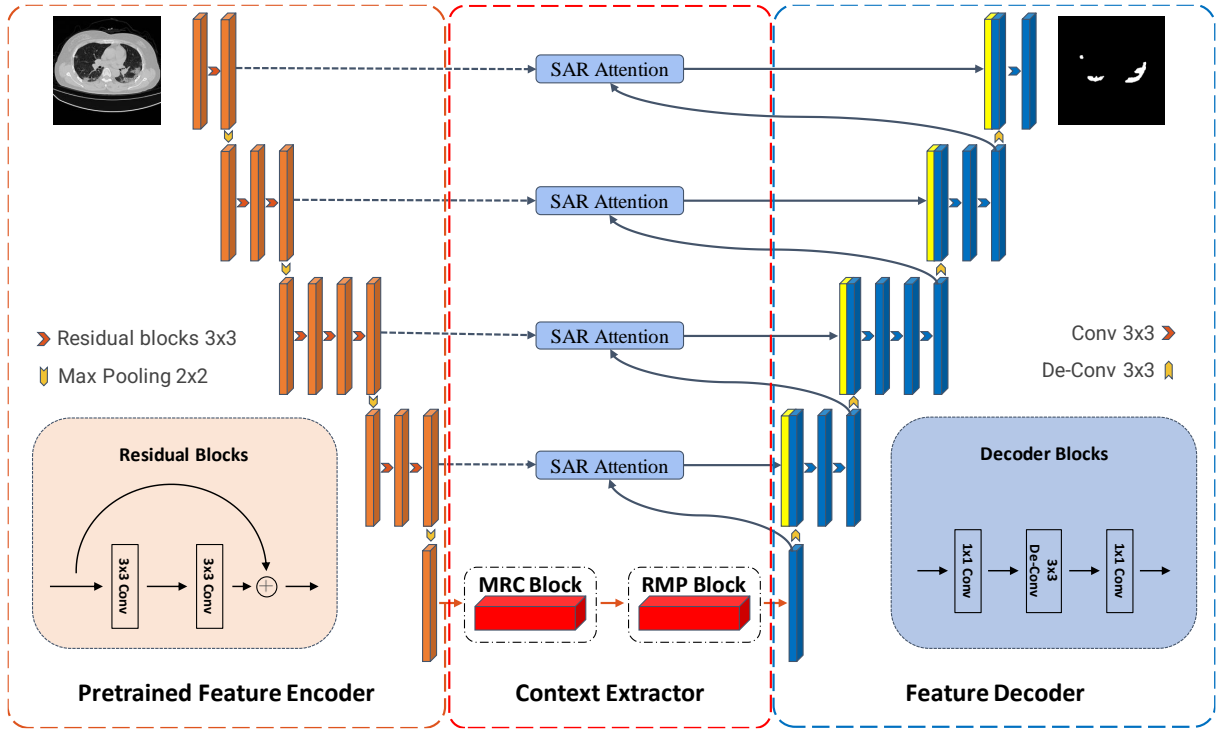


图 1. Illustration of our proposed network.

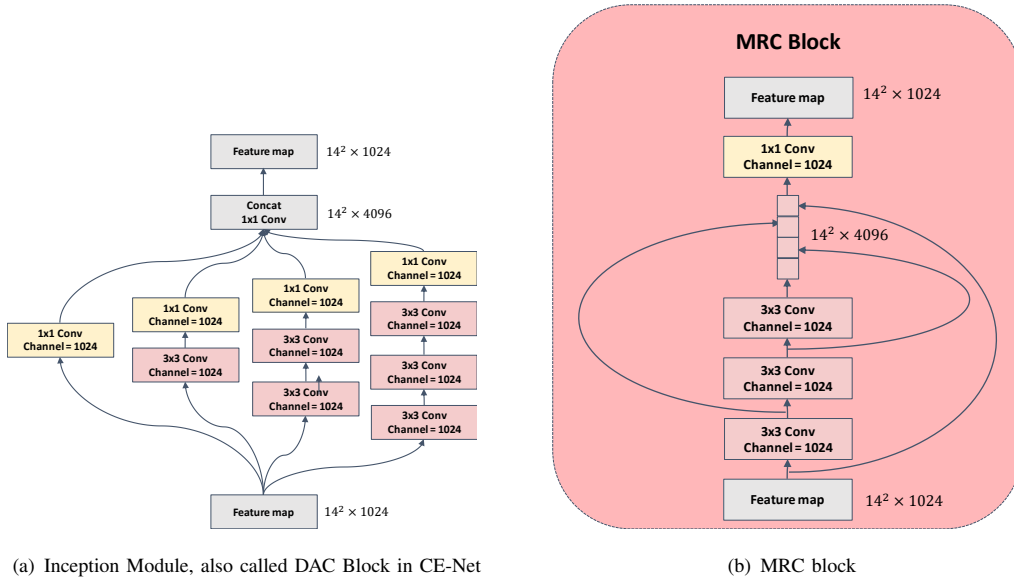


图 2. (2(a)) is the illustration of DAC Block. (2(b)) is the illustration of MRC Block.

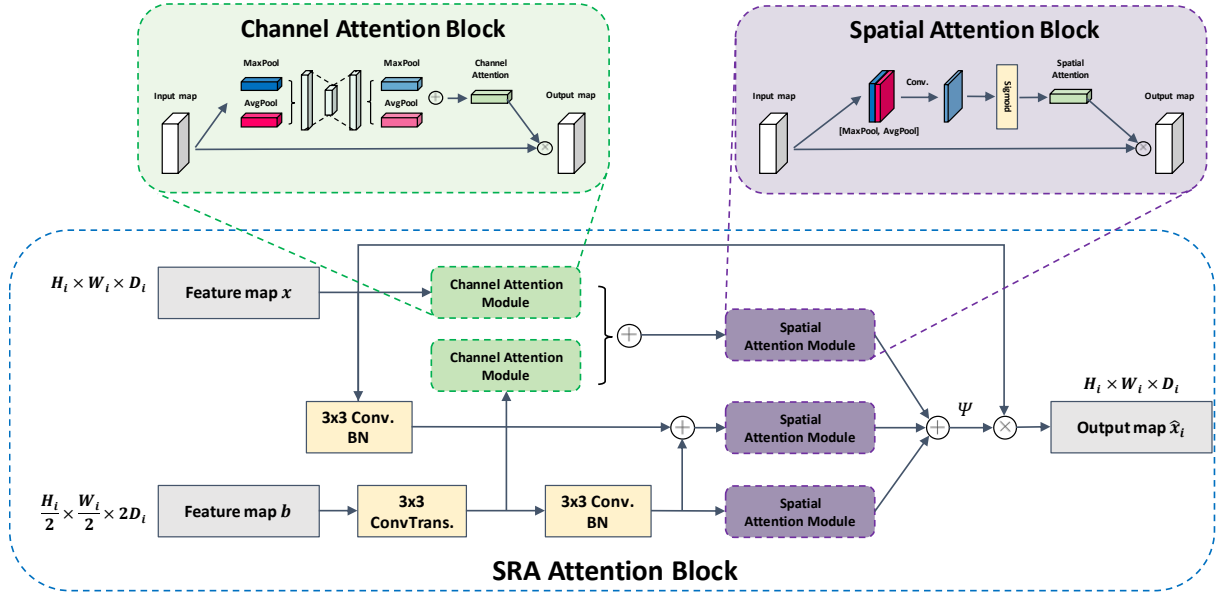


图 3. Illustration of SRA Attention Block.

2012. The data is a set of 30 images ( $512 \times 512$  pixels) from serial section transmission electron microscopy of the *Drosophila* first instar larva ventral nerve cord (VNC). Each image comes with a corresponding fully annotated ground truth segmentation map for cells (white) and membranes (black).

b: Liver

Liver tumor Segmentation Challenge (LiTS) [3] contain 131 contrast-enhanced CT images provided by hospital around the world with  $512 \times 512$  resolution. The ground truth segmentation provides two different labels: liver and lesion. For our experiments, we only consider liver as positive class and others as negative class.

c: COVID19

Dataset [5] includes whole volumes and includes, therefore, both positive and negative slices (373 out of the total of 829 slices have been evaluated by a radiologist as positive and segmented). Dataset [6] contains 20 CT scans of patients diagnosed with COVID-19 as well as segmentations of lungs and infections made by experts. These volumes are converted and normalized in a similar way as above, meanwhile we resize the data to  $512 \times 512$ .

### C. EVALUATION METRICS

The experiments are implemented using the Pytorch framework. We use Adam optimizer [7] as our models' optimizer with a learning rate of 0.00001, batch size of 2. All of datasets are splitted into training set, validation set and test set with the ratio of 8:1:1 using sklearn library. To numerically evaluate, we use five widely adopted metrics, *i.e.*, the Dice similarity coefficient(Dice.), F1 score., Sensitivity(Sen.), Iou. and hausdorff distance(Hd)., the expressions of them are defined as follows:

$$\text{Sensitivity} = \frac{TP}{TP + FN} \quad (1)$$

$$\text{DSC}(G, S) = \frac{2|G \cap S|}{|G| + |S|} \quad (2)$$

$$\text{IOU}(G, S) = \frac{|G \cap S|}{|G| \cup |S|} \quad (3)$$

$$F_1 = 2 \cdot \frac{\text{precision} \cdot \text{recall}}{\text{precision} + \text{recall}} \quad (4)$$

$$h(G, S) = \max_{g \in G} \left\{ \min_{c \in C} \|g - c\| \right\} \quad (5)$$

### D. MEDICAL IMAGE SEGMENTATION RESULTS

For comparison, we use five original network FCN with 32s [8], U-Net [9], U-Net++ [10], CE-Net [1] and U-Net with Attention Gate [11] to evaluate our proposed method.

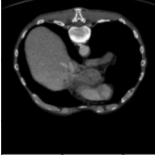

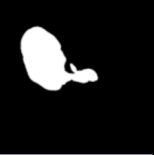



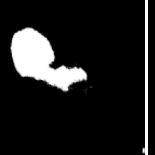

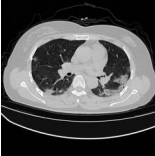

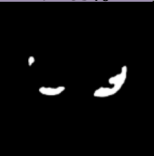








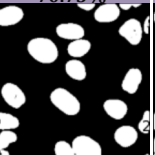
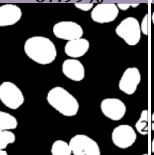
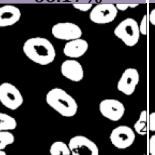
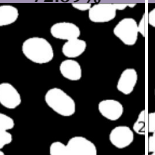
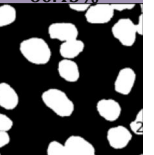
	Img	GT	Our Method	Att U-Net	U-Net++	U-Net	CE-Net	FCN32s
Liver								
COVID19								
DSB Cell								
			91.65%	87.76%	87.81%	86.15%	87.21%	83.00%
			74.57%	70.73%	67.99%	66.17%	72.69%	60.45%
			89.65%	87.76%	87.81%	86.15%	87.21%	83.00%

图 4. Medical image segmentation examples.

我们利用U-Net, ResU-Net作为baseline, 与我们提出的模型分别在Cell, Liver, COVID19三个数据集上进行对比, 每次实验所使用的参数, 训练集, 验证集, 测试集均相同。

#### 1) Live segmentation results

Segmentation results of cell segmentation are shown in tables III-D1, 在Dice. and F1 score指数上相比于 CE-Net, U-Net++, U-Net with Attention Gate, U-Net and FCN32s分别提升了1.30%, 1.49%, 4.35%, 6.11% and 16.95%. 在Iou.指数上, 分别提升了2.05, 2.27%, 6.08%, 7.30% and 19.70%. 在Sens.指数上分别提升了9.80%, 6.53%, 7.39%, 11.81% and 15.36%. 在Hd.指数上分别降低了0.4074, 0.9083, 0.7471, 0.8825 and 2.4968.

#### 2) Cell segmentation results

Segmentation results of cell segmentation are shown in table III-D1, 在Dice. and F1 score指数上相比于 CE-Net, U-Net++, U-Net with Attention Gate, U-Net and FCN32s分别提升了2.01%, 2.05%, 2.36%, 2.98% and 4.86%. 在Iou.指数上, 分别提升了3.84%, 3.89%, 4.44%, 5.50% and 8.65%. 在Sens.指数上分别提升了2.33%, 3.33%, 3.44%, 2.83% and 0.08%. 在Hd.指数上分别降低了1.9362, 0.9506, 1.0186, 2.7931 and 4.0846.

#### 3) COVID19 segmentation results

Segmentation results of covid19 segmentation are shown in table III-D1, 在Dice. and F1 score指数上相比于 CE-Net, U-

Net++, U-Net with Attention Gate, U-Net and FCN32s分别提升了1.41%, 4.75%, 2.60%, 6.15% and 10.80%. 在Iou.指数上, 分别提升了1.67%, 6.58%, 3.84%, 8.40% and 14.12%. 在Hd.指数上分别降低了0.4581, 0.7171, 0.5715, 0.9101 and 1.5514. 敏感度方面, 通过观察Figure 4我们可以发现, 其在分割目标图像时更加保守 (改)。

综上所述, 我们的模型在三个数据集上均consistently outperforms CE-Net and U-Net with Attention-Gate. Figure 4展示了我们在三个数据集上与其余5个模型的对比示例。COVID-19 ....., Liver ....., Cell .....

## IV. ABLATION STUDY

To justify the effectiveness of the pretrained U-Net [9], ResUNet [12], MRC(multi residual convolution) block, RMP block and SAR(spatial channel and gateway) Attention block in our proposed method, we conduct the following ablation study using the COVID19 and Cell dataset as examples.

### A. LOSS FUNCTION

为了验证我们使用的损失函数组合模型 $loss_{overall}$ 的有效性, 我们以自己设计的模型作为baseline, 在其他参数一致的情况下将其与 $loss_{BCE}$ 和 $loss_{BCE+Dice}$ 在COVID19数据集上进行对比,  $loss_{overall}$ 和 $loss_{BCE+Dice}$ 的定义如下所示:

$$loss_{overall} = \alpha loss_{BCE} + \beta loss_{Dice} + \theta loss_{ACE} \quad (6)$$

$$loss_{BCE+Dice} = \alpha loss_{BCE} + \beta loss_{Dice} \quad (7)$$

Datasets	Methods	Shape Loss	Dice.	F1 score.	Iou.	Sens.	Hd.
Cell	Our proposal	✓	<b>0.8588</b>	<b>0.8588</b>	<b>0.7623</b>	<b>0.9296</b>	<b>4.6224</b>
	CENet	×	0.8458	0.8458	0.7418	0.8316	5.2098
	UNet++	×	0.8439	0.8439	0.7396	0.8643	5.5307
	Attention UNet	×	0.8153	0.8153	0.7015	0.8557	5.3695
	UNet	×	0.7977	0.7977	0.6893	0.8115	5.5049
	FCN32s	×	0.6895	0.6895	0.5653	0.7760	7.1192
Liver	Our proposal	✓	<b>0.9551</b>	<b>0.9551</b>	<b>0.9165</b>	<b>0.9389</b>	<b>3.8854</b>
	U-Net++	×	0.9351	0.9351	0.8781	0.9156	5.8218
	Attention UNet	×	0.9346	0.9346	0.8776	0.9056	4.836
	CENet	×	0.9315	0.9315	0.8721	0.9045	4.904
	U-Net	×	0.9253	0.9253	0.8615	0.9106	6.6785
	FCN32s	×	0.9065	0.9065	0.8300	0.9381	7.97
COVID19	Our proposal	✓	<b>0.8489</b>	<b>0.8489</b>	<b>0.7457</b>	<b>0.8570</b>	<b>4.313</b>
	CENet	×	0.8348	0.8348	0.7290	0.9359	4.7711
	UNet++	×	0.8014	0.8014	0.6799	0.9426	5.0301
	Attention UNet	×	0.8229	0.8229	0.7073	0.9435	4.8845
	UNet	×	0.7874	0.7874	0.6617	0.9528	5.2231
	FCN32s	×	0.7409	0.7409	0.6045	0.9935	5.8644

表 3. Comparison With Other Methods In Cell [4], Liver [3] and COVID19 [6] Dataset

Methods	Loss	Dice.	F1 score.	Iou.	Sens.	Hd.
Our proposal	BCE	0.8076	0.8076	0.6874	0.8772	5.0112
Our proposal	BCE+DiceLoss	0.8375	0.8375	0.7282	0.8827	4.7241
Our proposal	Ours	0.8489	0.8489	0.7457	0.8570	4.4313

表 4. Comparison With Other loss functions In COVID19 [5] Dataset

在本次实验中，我们预先设置 $\alpha = 0.5, \beta = 0.5$ 。对于 $\theta$ ，因为ACEloss与图像梯度有关，其loss value的范围通常为 $[10^1, 10^5]$ ，所以 $\theta$ 值应该显著小于 $\alpha, \beta$ ，在本次试验中，我们预先设置 $\theta = 0.0005$ 。实验结果如表IV-A所示，对比于 $loss_{overall}$ 和 $loss_{BCE+Dice}$ ，在Dice.指标上我们分别提升了4.13%，1.14%；在F1 score.指标上我们分别提升了4.13%，1.14%；在Iou.指标上我们分别提升了5.83%，1.75%；在Sens.指标上我们分别降低了2.02%，2.57%；在Hd.指标上我们分别降低了0.5799，0.2928，其推理结果如图5所示。

## B. MODULES

为了进一步验证我们设计的各个模块是否对分割任务有提升作用，我们将MRC Block, RMP Block, SRA Attention Block和shape loss function与ResU-Net分别进行组合：

- ResU-Net + MRC + RMP: to verify if this blocks can

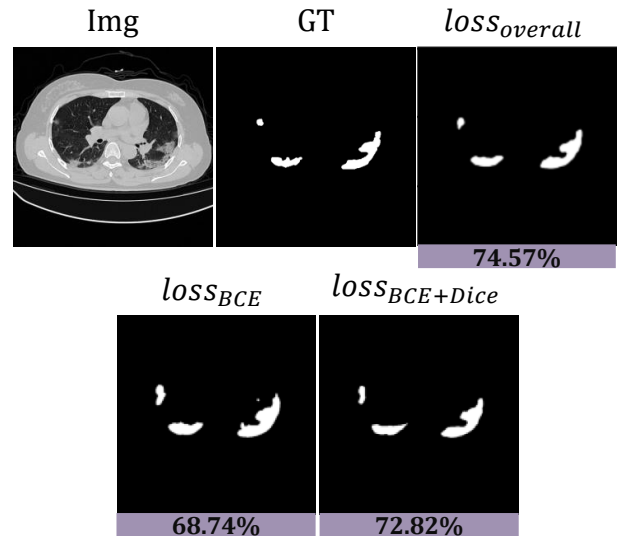


图 5. 不同损失函数训练下的模型推理结果

really 提升对深层图像特征的提取能力

- ResU-Net + SAR Attention Module: to verify if our Attention module can 更好地从spatial and channels角度enhanced pixel-wised segmentation than skip connection as well as attention-gate.
- ResU-Net + MRC + RMP +SAR: 分别使用 $loss_{BCE}$  and  $loss_{overall}$ 来进行训练, 用于验证组合模型的有效性。

#### a: COVID19 ablation study result

我们将上述模型在COVID19数据集上进行测试并对比其IoU, F1 score, Dice, Sensitivity and Hd value. 每次实验所使用的参数, 训练集, 验证集, 测试集均相同。如图6和表IV-B所示: ResU-Net with MRC block and RMP block 对比于ResU-Net,Iou.指标提升了1.40%, F1 score指标提升了1.34%, Dice指标提升了1.34%, Sensitivity指标提升了0.29%, Hd指标降低了0.5214。 ResU-Net with SRA attention module 对比于ResU-Net,Iou.指标提升了2.60%, F1 score指标提升了2.31%, Dice指标提升了2.31%, Sensitivity指标降低了0.16%, Hd指标降低了0.6260。 ResU-

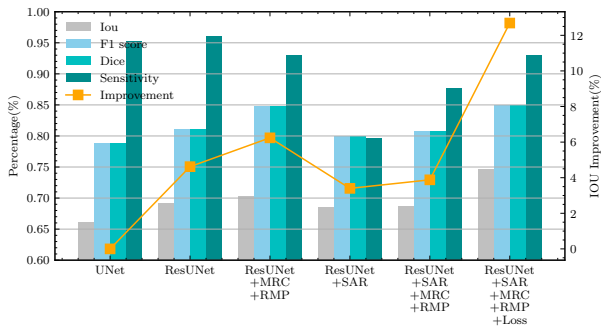


图 6. Metric results of COVID19 segmentation compared with different models.

Net with both SRA attention module and MRC, RMP module对比于ResU-Net,Iou.指标提升了3.24%, F1 score指标提升了2.11%, Dice指标提升了2.11%, Sensitivity指标提升了0.59%, Hd指标降低了0.6651。 ResU-Net with both SRA attention module and MRC with the combination of shape loss function, RMP module对比于ResU-Net,Iou.指标提升了3.49%, F1 score指标提升了2.74%, Dice指标提升了2.74%, Sensitivity指标降低了3.89%, Hd指标降低了0.9637。

#### b: Cell ablation study result

我们将上述模型在Cell数据集上进行测试并对比其IoU, F1 score, Dice, Sensitivity and Hd value. 每次实验所使

用的参数, 训练集, 验证集, 测试集均相同。如图7和表IV-B所示: ResU-Net with MRC block and RMP block 对比于ResU-Net,Iou.指标提升了1.40%, F1 score指标提升了1.34%, Dice指标提升了1.34%, Sensitivity指标提升了0.29%, Hd指标降低了0.5214。 ResU-Net with SRA attention module 对比于ResU-Net,Iou.指标提升了2.60%, F1 score指标提升了2.31%, Dice指标提升了2.31%, Sensitivity指标降低了0.16%, Hd指标降低了0.6260。 ResU-

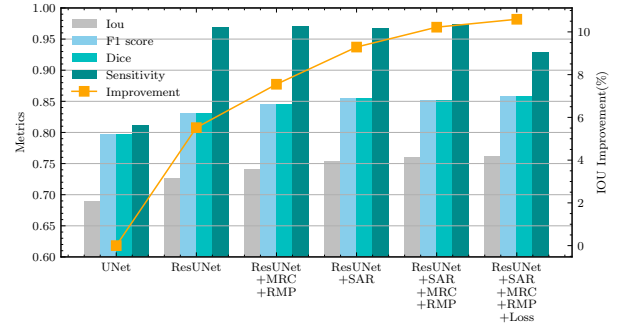


图 7. Metric results of Cell segmentation compared with different models.

Net with both SRA attention module and MRC, RMP module对比于ResU-Net,Iou.指标提升了3.24%, F1 score指标提升了2.11%, Dice指标提升了2.11%, Sensitivity指标提升了0.59%, Hd指标降低了0.6651。 ResU-Net with both SRA attention module and MRC with the combination of shape loss function, RMP module对比于ResU-Net,Iou.指标提升了3.49%, F1 score指标提升了2.74%, Dice指标提升了2.74%, Sensitivity指标降低了3.89%, Hd指标降低了0.9637。

Furthermore, 通过将上述模型的IoU指标进行对比, 我们可以发现相比于ResU-Net, both MRC+RMP module and SAR attention module 可以有效地提高模型的整体性能, 同时两者的结合也能起到不错的提升效果 (分别提升了 1.84%, 0.64%)。同时, 由于MRC block是CE-Net中DAC block的修改, 所以我们也该模型与CE-Net进行了对比, 在IoU识别率仅仅降低了0.04%的情况下, 我们的模型实现了30.17%的参数精简, 提高了训练的速度和节省了模型的显存消耗。

## V. CONCLUSION

## VI. ACKNOWLEDGMENT

### 参考文献

- [1] Z. Gu, J. Cheng, H. Fu, K. Zhou, H. Hao, Y. Zhao, T. Zhang, S. Gao, and J. Liu, "Ce-net: Context encoder network for 2d medical image segmentation," *IEEE Transactions on Medical Imaging*,



Dataset	Methods	Loss	Dice.	F1 score.	Iou.	Sens.	Hd.
COVID19	U-Net	BCE	0.7874	0.7874	0.6617	0.9528	5.2231
	ResU-Net	BCE	0.8105	0.8105	0.6923	0.9601	5.0248
	ResU-Net + MRC + RMP	BCE	0.8185	0.8185	0.7030	0.9295	4.8931
	ResU-Net + SAR	BCE	0.7988	0.7988	0.6846	0.7969	5.1522
	ResU-Net+SAR+MRC+RMP	BCE	0.8076	0.8076	0.6874	0.8772	5.0112
	ResU-Net+SAR+MRC+RMP	Ours	<b>0.8489</b>	<b>0.8489</b>	<b>0.7457</b>	<b>0.8570</b>	<b>4.313</b>
Cell	U-Net	BCE	0.7977	0.7977	0.6893	0.8115	5.5049
	ResU-Net	BCE	0.8314	0.8314	0.7274	0.9685	5.5861
	ResU-Net + MRC + RMP	BCE	0.8448	0.8448	0.7414	0.9714	5.0647
	ResU-Net + SAR	BCE	0.8545	0.8545	0.7534	0.9669	4.9601
	ResU-Net+SAR+MRC+RMP	BCE	0.8525	0.8525	0.7598	0.9744	4.9210
	ResU-Net+SAR+MRC+RMP	Ours	<b>0.8588</b>	<b>0.8588</b>	<b>0.7623</b>	<b>0.9296</b>	<b>4.6224</b>

表 5. Ablation study for each component on COVID19 and Cell dataset

- vol. 38, no. 10, p. 2281–2292, Oct 2019. [Online]. Available: <http://dx.doi.org/10.1109/TMI.2019.2903562>
- [2] I. Arganda-Carreras, S. C. Turaga, D. R. Berger, D. Cireşan, A. Giusti, L. M. Gambardella, J. Schmidhuber, D. Laptev, S. Dwivedi, J. M. Buhmann, T. Liu, M. Seyedhosseini, T. Tasdizen, L. Kamentsky, R. Burget, V. Uher, X. Tan, C. Sun, T. D. Pham, E. Bas, M. G. Uzunbas, A. Cardona, J. Schindelin, and H. S. Seung, “Crowdsourcing the creation of image segmentation algorithms for connectomics,” *Frontiers in Neuroanatomy*, vol. 9, p. 142, 2015. [Online]. Available: <https://www.frontiersin.org/article/10.3389/fnana.2015.00142>
- [3] P. Christ, “Lits – liver tumor segmentation challenge (lits17).” [Online]. Available: <https://competitions.codalab.org/competitions/17094>
- [4] J. C. Caicedo, A. Goodman, K. W. Karhohs, and B. A. Cimini, “Nucleus segmentation across imaging experiments: the 2018 data science bowl,” *Nature Methods*, vol. 16, no. 12, pp. 1247–1253, Dec 2019. [Online]. Available: <https://doi.org/10.1038/s41592-019-0612-7>
- [5] Websites, “Covid-19 ct segmentation dataset.” [Online]. Available: <https://medicalsegmentation.com/covid19/>
- [6] M. Jun, G. Cheng, W. Yixin, A. Xingle, G. Jiantao, Y. Ziqi, Z. Mingqing, L. Xin, D. Xueyuan, C. Shucheng, W. Hao, M. Sen, Y. Xiaoyu, N. Ziwei, L. Chen, T. Lu, Z. Yuntao, Z. Qiongjie, D. Guoqiang, and H. Jian, “COVID-19 CT Lung and Infection Segmentation Dataset,” Apr. 2020. [Online]. Available: <https://doi.org/10.5281/zenodo.3757476>
- [7] D. P. Kingma and J. Ba, “Adam: A method for stochastic optimization,” 2017.
- [8] J. Long, E. Shelhamer, and T. Darrell, “Fully convolutional networks for semantic segmentation,” *CoRR*, vol. abs/1411.4038, 2014. [Online]. Available: <http://arxiv.org/abs/1411.4038>
- [9] O. Ronneberger, P. Fischer, and T. Brox, “U-net: Convolutional networks for biomedical image segmentation,” *CoRR*, vol. abs/1505.04597, 2015. [Online]. Available: <http://arxiv.org/abs/1505.04597>
- [10] Z. Zhou, M. M. R. Siddiquee, N. Tajbakhsh, and J. Liang, “Unet++: Redesigning skip connections to exploit multiscale features in image segmentation,” 2020.
- [11] J. Schlemper, O. Oktay, M. Schaap, M. P. Heinrich, B. Kainz, B. Glocker, and D. Rueckert, “Attention gated networks: Learning to leverage salient regions in medical images,” *CoRR*, vol. abs/1808.08114, 2018. [Online]. Available: <http://arxiv.org/abs/1808.08114>
- [12] F. I. Diakogiannis, F. Waldner, P. Caccetta, and C. Wu, “Resunet-a: A deep learning framework for semantic segmentation of remotely sensed data,” *ISPRS Journal of Photogrammetry and Remote Sensing*, vol. 162, p. 94–114, Apr 2020. [Online]. Available: <http://dx.doi.org/10.1016/j.isprsjprs.2020.01.013>



HAO LI is currently pursuing his bachelor's with the College of Information Science and Technology, Beijing University of Chemical Technology, Beijing.

His research interest include robotics, computer vision and deep learning.



SECOND B. AUTHOR was born in Greenwich Village, New York, NY, USA in 1977. He received the B.S. and M.S. degrees in aerospace engineering from the University of Virginia, Charlottesville, in 2001 and the Ph.D. degree in mechanical engineering from Drexel University, Philadelphia, PA, in 2008.

From 2001 to 2004, he was a Research Assistant with the Princeton Plasma Physics Laboratory. Since 2009, he has been an Assistant Professor with the Mechanical Engineering Department, Texas A&M University, College Station. He is the author of three books, more than 150 articles, and more than 70 inventions. His research interests include high-pressure and high-density nonthermal plasma discharge processes and applications, microscale plasma discharges, discharges in liquids, spectroscopic diagnostics, plasma propulsion, and innovation plasma applications. He is an Associate Editor of the journal *Earth, Moon, Planets*, and holds two patents.

Dr. Author was a recipient of the International Association of Geomagnetism and Aeronomy Young Scientist Award for Excellence in 2008, and the IEEE Electromagnetic Compatibility Society Best Symposium Paper Award in 2011.

• • •